Rotavirus capsid VP6 tubular and spherical nanostructures act as local adjuvants when co-delivered with norovirus VLPs

M. Malm, S. Heinimäki, T. Vesikari and V. Blazevic [ID]

Vaccine Research Center, University of Tampere, Tampere, Finland

Summary

A subunit protein vaccine candidate based on norovirus (NoV) virus-like particles (VLPs) and rotavirus (RV) VP6 protein against acute childhood gastroenteritis has been proposed recently. RV VP6 forms different oligomeric nanostructures, including tubes and spheres when expressed *in vitro,* which are highly immunogenic in different animal models. We have shown recently that recombinant VP6 nanotubes have an adjuvant effect on immunogenicity of NoV VLPs in mice. In this study, we investigated if the adjuvant effect is dependent upon a VP6 dose or different VP6 structural assemblies. In addition, local and systemic adjuvant effects as well as requirements for antigen co-delivery and co-localization were studied. The magnitude and functionality of NoV GII.4-specific antibodies and T cell responses were tested in mice immunized with GII.4 VLPs alone or different combinations of VLPs and VP6. A VP6 dose-dependent adjuvant effect on GII.4-specific antibody responses was observed. The adjuvant effect was found to be strictly dependent upon co-administration of NoV GII.4 VLPs and VP6 at the same anatomic site and at the same time. However, the adjuvant effect was not dependent on the types of oligomers used, as both nanotubes and nanospheres exerted adjuvant effect on GII.4-specific antibody generation and, for the first time, T cell immunity. These findings elucidate the mechanisms of VP6 adjuvant effect in vivo and support its use as an adjuvant in a combination NoV and RV vaccine.

Keywords: adjuvant, nanospheres, nanotubes, norovirus VLP, rotavirus VP6

Introduction

Noroviruses (NoV) and rotaviruses (RV) are the most common causes, at a very young age, of childhood viral gastroenteritis (GE) worldwide [1–3]. To eliminate the high risk of NoV and RV-caused gastroenteritis (GE), a vaccination soon after birth would be needed. Nevertheless, NoV infections and disease are not yet preventable by vaccination, although NoV virus-like particles (VLPs)-based vaccines are being studied extensively. NoV VLPs are non-infectious self-assembled particles composed of VP1 capsid protein, highly resembling intact virions both structurally and antigenically [4]. Currently used RV vaccines are based on live attenuated viruses [5,6] that are associated with potential safety issues, such as a risk of intussusception [7] and shedding and transmission of the vaccine strains and reassortment to yield more virulent forms [8], supporting the need for non-live RV subunit vaccines. Our group has recently developed a

combination vaccine candidate against NoV and RV childhood GE consisting of NoV VLPs and RV VP6 [9,10]. The combination vaccine induced strong type-specific and cross-reactive humoral and cellular immunity against NoV and RV in a mouse model [9,11–13].

In general, highly purified subunit vaccines with the best safety profile have poor immunogenicity, and the magnitude and quality of the immune responses need to be enhanced by adjuvants [14]. However, due to the vulnerability of infants and young children, it would be highly desirable to have an efficient vaccine without adding external adjuvants [15,16]. To this end, we have shown that RV VP6 not only induced protective immunity against live RV challenge in mice [13], but it also acted as a strong *in-vivo* adjuvant on the generation of antibodies specific for NoV [17].

In a triple-layered RV particle the intermediate layer is formed by the VP6 protein (45 kD), situated between the
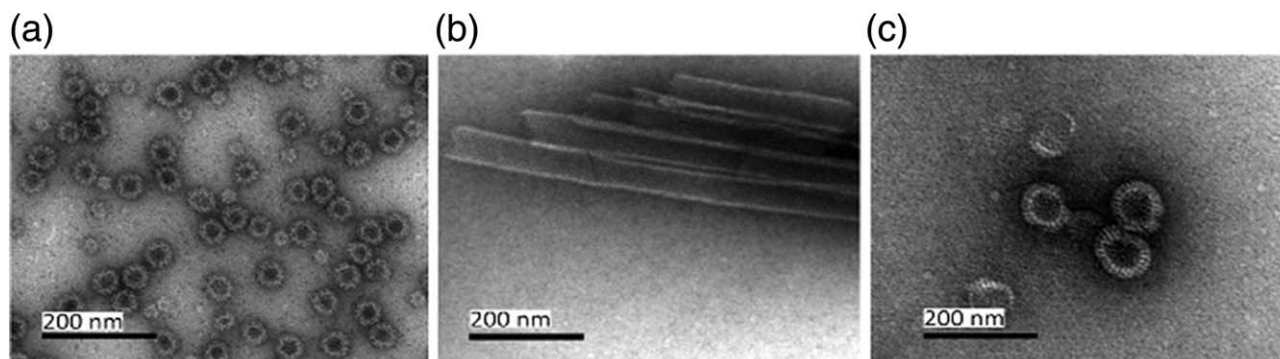
(a) (b) (c)

Fig. 1. Structure and integrity of the proteins. Electron microscopy images of baculovirus–insect cell system-produced norovirus (NoV) GII.4-1999 virus-like particles (VLPs) (a), rotavirus (RV) VP6 nanotubes (b) and VP6 nanospheres (c) examined by FEI Tecnai F12 electron microscope (Philips Electron Optics) after negative staining with 3% uranyl acetate, pH 4·6. Images observed at ×23 000 (a,c) or ×6800 (b) magnification.

outermost layer consisting of VP4 and VP7 proteins and the inner core protein VP2, which surrounds the double-stranded genome of RV [6,18,19]. RV VP6 is the most abundant and immunogenic RV protein [20,21], which is highly conserved among RV strains [22,23]. VP6 forms trimers organized into hexagons and packed into higher-order structural assemblies, e.g. VP6 nanotubes (VP6T) and nanospheres (VP6S), when expressed *in vitro* [12,24–27] under different conditions [25,28]. The rVP6 is highly immunogenic [9,12,29], and it has also been used as a carrier or delivery platform for heterologous protein anti-gens and genetically fused epitope-based vaccines, with improved response to the foreign antigen [30–34]. VP6 is stable at different pH conditions, and when delivered orally it was targeted to intestinal cells, offering a promising new delivery platform to transport pharmaceutical compounds to gastrointestinal tract [35].

In order to elucidate the mechanisms of VP6 adjuvant action, we have shown previously that VP6T are taken up efficiently by macrophages and dendritic cells (DC) *in vitro*, resulting in activation and maturation of these antigen-presenting cells (APC). Also, VP6T were shown to facilitate the internalization of co-delivered NoV VLPs to the APC [36]. We undertook the present study to investigate requirements for co-localization and co-delivery of the rVP6 with the NoV VLPs *in vivo* and whether VP6 works as a local or systemic adjuvant. In addition, adjuvant effect of VP6T was compared to VP6S.

Materials and methods

Recombinant proteins

NoV VLPs and RV VP6 oligomeric proteins were produced in a baculovirus–insect cell expression system, as described in detail elsewhere [9,12,37]. NoV GII.4-1999 VLPs (GenBank reference strain, Accession number AF080551) and rVP6 antigens (Accession no. GQ477131) used for immunizations of animals were highly purified with multi-step chromatographic procedures or various steps of ultra-filtration, as described previously [17,38]. The purified rVP6 was assembled into nanotubes in phosphate-buffered saline (PBS) at pH 7·3–7·5 (Lonza, Verviers, Belgium) or nanospheres in a 50 mM sodium acetate buffer with 130 mM NaCl, pH 4·82 [38]. The concentration of the proteins was determined using Pierce BCA protein assay (Thermo Scientific, Waltham, MA, USA). The purity of the proteins was verified by Quant-it dsDNA Broad-Range Assay Kit (Invitrogen, Carlsbad, CA, USA; < 10 ng dsDNA/10 μg of protein), sodium dodecyl sulphate poly-acrylamide gel electrophoresis (SDS-PAGE), BacPAK Rap-idTiter Kit [Clontech Laboratories, Mountain View, CA, USA; 0 plaque-forming units (pfu) live BV/ml] and limulus amebocyte lysate assay (Lonza, < 0·1 endotoxin units/100 μg of protein), as described in detail elsewhere [9,38]. The VLPs and oligomeric rVP6 nanostructures used for immu-nizations were confirmed by negative-staining transmission electron microscopy (TEM) using an FEI Tecnai F12 (Philips Electron Optics, Eindhoven, the Netherlands) after negative staining with 3% uranyl acetate pH 4·6 for protein morphology and integrity (Fig. 1a–c). NoV VLPs used for enzyme-linked immunosorbent assay (ELISA)-based ana-lytical methods, GII.4-1999, GII.4 New Orleans (NO) 2009 (Accession no. GU445325) and GII.4 Sydney (SYD) 2012 (Accession no. AFV08795.1) were purified using sucrose gradient ultracentrifugation, as described elsewhere [37].

Synthetic peptides and viruses

For quantification of NoV-specific T cell responses by enzyme-linked immunospot (ELISPOT), an interferon (IFN)-γ assay GII.4 peptide pool (Synpeptide Co. Ltd, Shanghai, China) containing 76 synthetic peptides [18-mers, 11 amino acid (aa) overlap], spanning the entire 539aa sequence of GII.4-1999 NoV VP1 [39], was used. VP6-specific BALB/c mouse (H-2^d) CD4$^+$ T cell epitope ^{242}DGATTWYFNPVILRPNNV^{259} [11,40], named R6-2, was synthetized (Proimmune Ltd, Oxford, UK) and used

Table 1. Experimental and control immunization groups

Group	Dose of GII.4 VLP	Dose and form of rVP6	Administration
I	0·3 µg	–	i.m.
II	0·3 µg	1 µg VP6T	i.m., co-administration
III	0·3 µg	10 µg VP6T	i.m., co-administration
IV	0·3 µg	30 µg VP6T	i.m., co-administration
V	0·3 µg	10 µg VP6T	i.m., VP6 first followed by the VLP after 1 h
VI	0·3 µg	10 µg VP6T	i.m., left tight VP6, right tight VLP, at the same time
VII	0·3 µg	10 µg VP6S	i.m., co-administration
VIII	3 µg	–	i.m.
IX (Ctrl)	–	–	i.m., carrier only (PBS)

VLP = virus-like particle; rVP6 = recombinant VP6; i.m. = intramuscular; VP6T = VP6 nanotubes; VP6S = VP6 nanospheres; Ctrl = control; PBS = phosphate-buffered saline.

in RV VP6-specific ELISPOT assays. Ovalbumin (OVA) 323–339 chicken egg albumin peptide (aa [323]ISQAVHAA-HAEINEAGR[339], cat. #vac-isq; Invivogen, San Diego, CA, USA) served as a negative control.

For RV-specific ELISPOT assays human RV strains Wa (G1P1A[8]) and bovine RV strain WC3 (G6P7[5]) were propagated in fetal rhesus monkey kidney (MA104) cells, as described previously [12], and Ridascreen® Rotavirus kit (R-Biopharm AG, Darmstadt, Germany; cat. C0901) with the internal rVP6 standard was used to determine the VP6 amount (ng/ml) in the cultures.

Immunization of animals

Female 7–8-week-old BALB/c mice obtained from Envigo Laboratories (Horst, Limburg, the Netherlands) were divided to nine groups (groups I–IX) and immunized intramuscularly (i.m.) at study weeks 0 and 3 with different doses of antigens diluted in 50 µl PBS, as shown in Table 1. A minimum of five mice in each group was used. All antigens were delivered into the right thigh muscle of each mouse except group VI, which received GII.4 VLPs at the right thigh and VP6T at the contralateral left limb site at the same time. For immunizing groups II–IV and VII, the VLPs and VP6 were mixed prior to administration. To define the temporal requirements of VP6 adjuvant activity, mice in group V received 10 µg VP6T first, followed by 0·3 µg VLP 1 h later at the same site. Naive mice receiving carrier only (group IX) were used as negative controls. Animals were anaesthetized before immunization with sevoflurane inhalate and for euthanasia with a mixture of medetomidine (Dorbenevet, 1 mg/ml; Laboratorios SYVA SA, Leon, Spain) and ketamine (Ketaminol vet, 50 mg/ml; Intervet International BV, Boxmeer, the Netherlands). Blood and spleens were collected at the time of termination (at week 5) for the analysis of serological and cell-mediated immune responses, as described previously [41]. Serum samples were stored at −20°C, and spleen cell suspensions were stored in liquid nitrogen before use in the assays. All mice used were negative for NoV GII.4-specific immunoglobulin (Ig)G antibodies prior to the immunizations at week 0 (data not shown). Mice welfare was monitored throughout the study and experiments were performed in accordance with the guidelines of the Finnish National Animal Experiment Board.

Serum IgG antibody ELISA

Sera of immunized and control mice were analysed individually by ELISA to determine NoV GII.4-1999, GII.4-NO, GII.4 SYD and rVP6-specific IgG, IgG1 and IgG2a titres, as described previously [9,11]. Briefly, 96-well plates (Corning Inc. Corning, NY, USA) were coated with 50 ng/well of NoV VLPs or rVP6 in PBS. Duplicates of twofold serial dilutions of serum samples were incubated for 2 h at room temperature and bound antibodies were detected with horseradish peroxidase (HRP)-conjugated goat anti-mouse IgG (Sigma-Aldrich, St Louis, MO, USA), IgG1 (Invitrogen) or IgG2a (Invitrogen). Optical density (OD) at 490 nm was measured by a microplate reader Victor[2] 1420 (Perkin Elmer, Waltham, MA, USA) and a sample was considered positive if the OD was above the mean OD of control mice +3 standard deviations (s.d.) and > 0·1. End-point titres were expressed as the highest serum dilution giving a positive reading.

Blocking assay (a surrogate neutralization assay)

To examine the ability of serum antibodies to block the binding of NoV VLPs to a putative cellular histo-blood group antigen (HBGA) receptor, two different sources of HBGAs, pig gastric mucin (PGM) type III (Sigma Chemicals, St Louis, MO, USA) and human type A saliva were utilized [42,43]. The blocking assays were conducted with the procedures described in detail elsewhere [44]. Briefly, groupwise pooled twofold serum dilutions were preincubated with the 0·1 µg/ml GII.4-1999 VLPs and the mixtures were added to 96-microwell plates coated with 2·5 µg/ml PGM or 1 : 3000 diluted human type A saliva. Maximum

VLP binding signal (OD) was determined in wells lacking serum. The bound VLPs were detected using human anti-NoV detection serum and anti-human IgG conjugate (Novex; Thermo Fisher Scientific, Fremont, CA, USA). Blocking index was calculated as follows: $100\% - [OD$ (wells with serum)/OD (wells without serum, maximum binding)] $\times$ 100%. Results are expressed as the blocking titre 50 (BT_{50}), a serum titre blocking $\geq 50\%$ of the VLPs binding to the HBGAs [45].

Norovirus-specific ELISPOT IFN-γ

To quantify NoV GII.4-specific IFN-γ-producing T cells of immunized mice, an ELISPOT assay was used [11]. Splenocytes from either individual or groupwise pooled mice were plated on MultiScreenHTS-IP filter plates (Millipore, Billerica, MA, USA) coated with an anti-mouse IFN-γ monoclonal antibody (Mabtech AB, Nacka Strand, Sweden) at 5 μg/ml and blocked with 10% fetal bovine serum (FBS; Sigma-Aldrich). Cells were stimulated with GII.4-99 peptide pool (2 μg/ml), GII.4-99 VLPs (5 μg/ml) or OVA peptide (negative control, 4 μg/ml). Cells incubated in culture medium (CM) only (RPMI 1640 supplemented with 10% fetal bovine serum, 100 U/ml penicillin, 100 μg/ml streptomycin, 50 μM 2-mercaptoethanol and 2 mM L-glutamine; Sigma-Aldrich) and cells were stimulated with 10 μg/ml of T cell mitogen concanavalin A (ConA; Sigma-Aldrich, cat. C5275) served as a background and viability control. After overnight incubation (16–20 h) IFN-γ was detected with biotinylated anti-mouse IFN-γ monoclonal antibody (Mabtech AB, cat. 3321–6) and streptavidin–alkaline phosphatase (ALP) conjugate (Mabtech AB, cat. 3310–10). The spots were developed with BCIP/NBT (5-bromo-4-chloro-3-indolyl-phosphate) substrate (Mabtech AB, cat. 3650–10) and counted by ImmunoSpot® automatic CTL analyser (CTL-Europe GmbH, Bonn, Germany). The results were expressed as mean spot-forming cells (SFC)/10^6 splenocytes of duplicate wells. A positive result was considered as an increase of twice or more above the control antigen SFC counts. Background counts never exceeded 20 SFC/10^6 cells.

RV VP6-specific IFN-γ and IL-4 ELISPOT

VP6-specific IFN-γ and interleukin (IL)-4 T cell responses were tested using an ELISPOT assay stimulating the splenocytes of immunized and control mice with rVP6 protein (5 μg/ml), R6-2 peptide (5 μg/ml), RV Wa, RV WC3 (0·5 μg VP6/ml) or MA104 mock antigen. IFN-γ ELISPOT assay was performed similarly to NoV-specific ELISPOT IFN-γ, as described above. For quantification of IL-4 production the MultiScreenHTS-IP filter plates were coated with anti-mouse IL-4 monoclonal antibody (Mabtech AB, cat. 3311-3) at 5 μg/ml. Groupwise pooled cells were plated and incubated with the antigens for 40–45 h. Biotinylated anti-mouse IL-4 antibody (Mabtech AB, cat. 3311-6) followed by incubation with streptavidin–ALP and BCIP/NBT substrate were used for developing the spots. The spots were counted and the results were expressed as described above.

Statistics

The statistical differences between independent groups were assessed by Mann–Whitney *U*-test for serum IgG end-point titres and ELISPOT assay results. Wilcoxon's signed-rank test for comparing two related samples was used for analysing the difference between IgG1 and IgG2a end-point titres. Statistical analyses were performed using IBM SPSS statistics (SPSS, Chicago, IL, USA) version 23. $P < 0.05$ was considered statistically significant.

Results

VP6 adjuvant effect on NoV-specific serum antibody responses is dose-dependent

In order to determine the mechanism of adjuvant effect of RV VP6 on NoV-specific antibody responses, mice were immunized with a suboptimal dose (0·3 μg) of GII.4-1999 VLP alone or co-administered with different doses of rVP6T. Immunization with 0·3 μg GII.4 VLP did not elicit a significant serum IgG response, whereas co-administration of 0·3 μg GII.4 VLP with 10 μg VP6T resulted in robust NoV-specific serum IgG levels (Fig. 2a), confirming our previous observation [17]. The GII.4-specific serum IgG titres were similar ($P = 0.853$) to the titres obtained with a 3 μg dose of GII.4 VLP alone used as a positive control (Fig. 2a, group VIII). A 1 μg dose of VP6T co-administered with 0·3 μg GII.4 VLP induced lower antibody responses than a 10 μg dose of VP6T (Fig. 2a, groups II and III, $P < 0.01$), while a 30 μg dose induced similar responses (Fig. 2a, groups III and IV, $P = 0.425$), indicating that the VP6 adjuvant effect was dose-dependent, but plateaued after maximum effect.

VP6 adjuvant effect on NoV-specific serum antibody responses is local and requires co-delivery

The spatial and temporal requirements of rVP6 adjuvant activity were next evaluated. A requirement for co-administration of 0·3 μg GII.4 VLP + 10 μg VP6T was tested by delivering antigens at the same time as a mixture (Table 1, group III), delivering the VLPs 1 h following the VP6T at the same site (Table 1, group V) or delivering antigens at the same time at the contralateral sites (Table 1, group VI). Co-administration as a mixture induced significantly higher serum NoV GII.4-specific IgG than injecting VP6T and GII.4 VLPs separately into the same site with 1 h difference (Fig. 2a, groups III and V, $P = 0.005$). Remarkably, no VP6 adjuvant effect on GII.4-specific serum IgG was seen when the antigens were spatially dissociated (Fig. 2a, groups III and VI, $P < 0.005$). Hence, the adjuvant
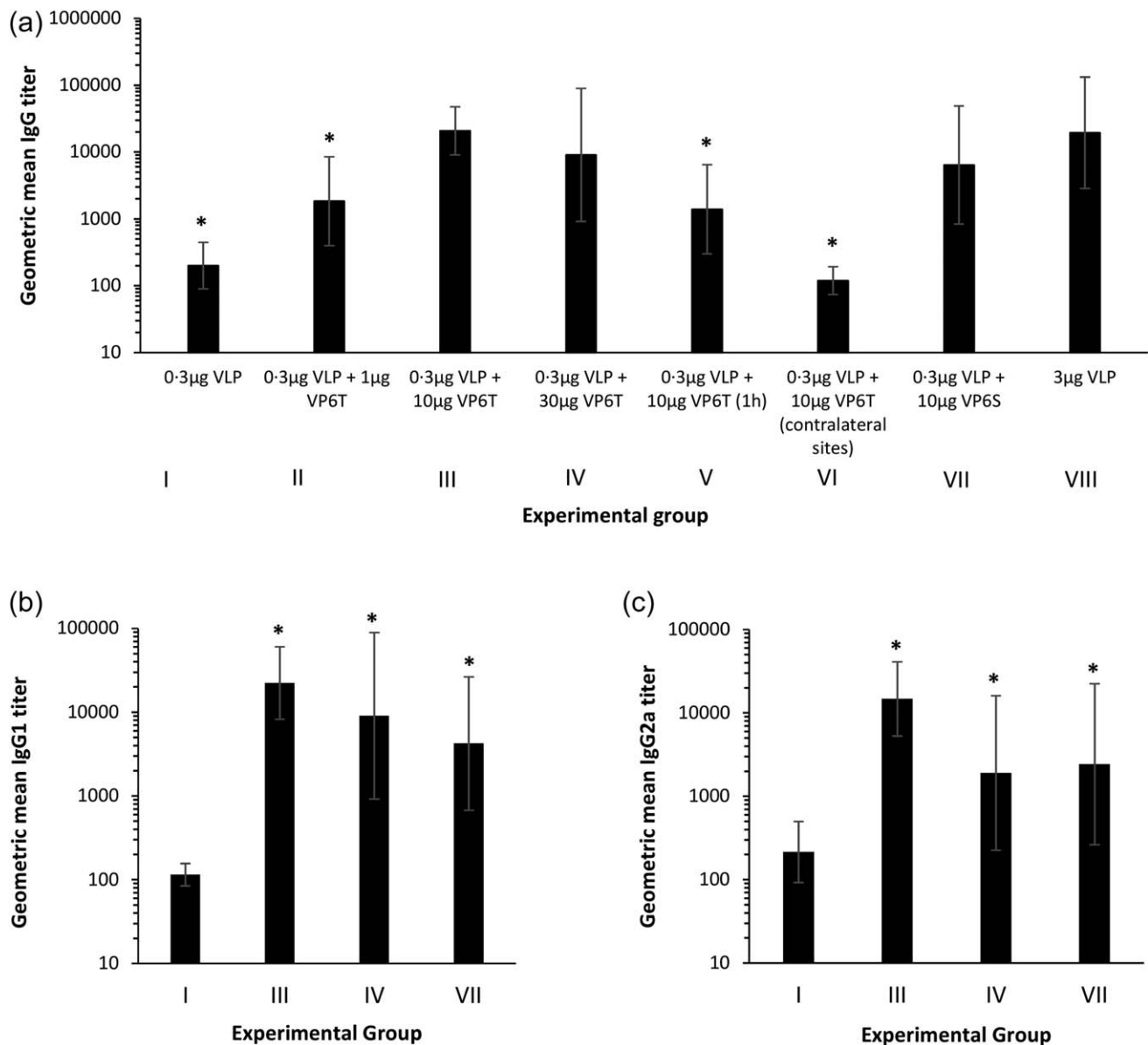
Fig. 2. GII.4 genotype-specific immunoglobulin (Ig)G antibody titres. IgG (a), IgG1 (b) and IgG2a (c) end-point titres were determined from individual, serially diluted sera of immunized mice in enzyme-linked immunosorbent assay (ELISA). Bars represent $\log_{10}$ geometric mean titres with 95% confidence intervals. For negative mice sera, an arbitrary titre of 1 : 100 (half the starting serum dilution, 1 : 200) was assigned. *Significantly different ($P < 0.05$) antibody titres compared to group III (a) or compared to group I (b,c).

effect of rVP6 is apparently exerted locally at the site of administration and not systemically.

VP6 adjuvant effect on NoV-specific serum antibody responses is not dependent upon the type of oligomeric structures

We further determined if there is a difference in VP6 adjuvant effect induced with VP6T or VP6S, as both tubular as well as spherical structures were shown previously to be highly immunogenic in mice [12]. When 10 µg VP6S were co-delivered with the VLPs instead of the VP6T,

comparable IgG titres were observed ($P = 0.211$) (Fig. 2a), indicating that both oligomeric conformational structures of rVP6 have comparable adjuvant ability. All negative control mice receiving PBS only were negative for NoV GII.4-specific antibodies (data not shown).

VP6 promotes unbiased Th1/Th2-type responses

To determine if the rVP6 has an adjuvant effect on NoV GII.4-specific T helper type 1 (Th1)-type and/or Th2-type responses, experimental groups where the VP6 adjuvant effect was seen (Fig. 2a, groups III, IV and VII, respectively)
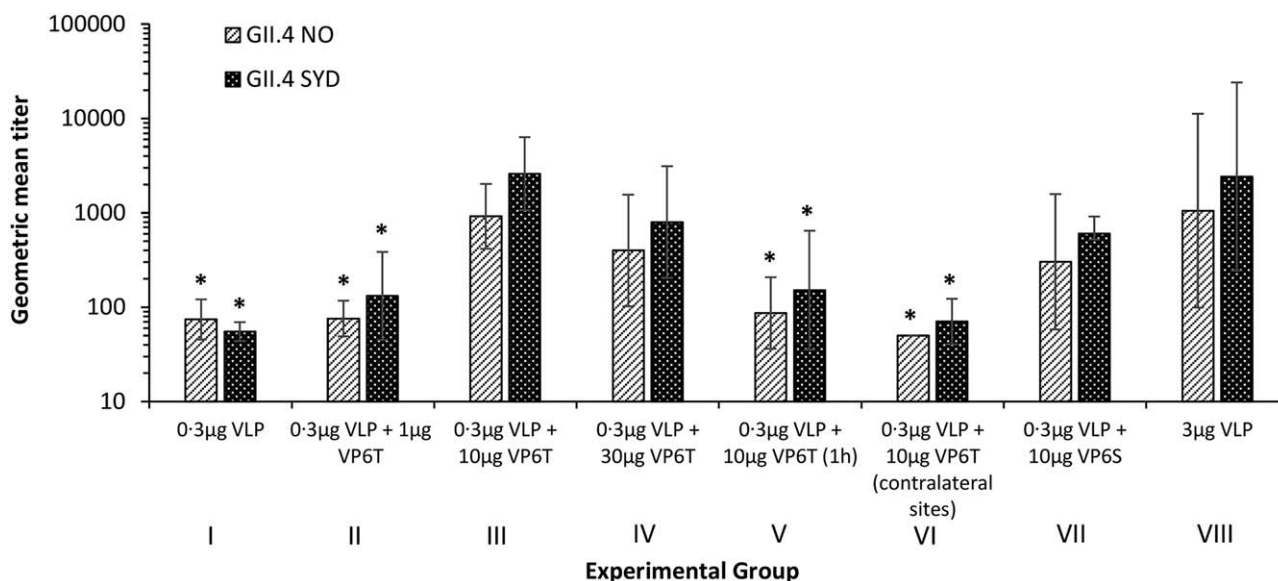
Fig. 3. Norovirus (NoV) cross-reactive immunoglobulin (Ig)G antibodies. Individual, serially diluted sera of immunized mice were analysed for cross-reactive anti-GII.4 New Orleans (NO) and anti-GII.4 Sydney (SYD) IgG end-point titres. An arbitrary end-point titre of 50 (half the starting dilution, 1 : 100) was assigned for negative mice sera. Bars represent $\log_{10}$-expressed geometric mean titres of each group with 95% confidence intervals. *Significantly different ($P < 0.05$) antibody titres compared to group III.

were tested for GII.4-specific IgG1 and IgG2a antibody subtypes. Both GII.4-specific IgG1 (Fig. 2b) and IgG2a antibodies (Fig. 2c) were detected congruently to the IgG responses seen in Fig. 2a, with significantly higher end-point titres induced when VP6 was co-administered with 0·3 µg VLP ($P < 0.05$ for all). There were no significant differences in the subtype-specific serum end-point titres observed ($P = 0.125$), indicating balanced Th1- and Th2-type responses.

VP6 adjuvant effect on NoV-specific cross-reactive and blocking antibodies

The VP6 adjuvant effect on cross-reactive serum IgG titres against two different variants of NoV GII.4 VLPs, GII.4

NO-2010 and GII.4 SYD-2012 VLPs was also investigated (Fig. 3). Cross-reactive IgG antibodies following immunization with 0·3 µg GII.4 VLPs were improved significantly ($P < 0.005$) by co-administration with 10 µg (group III) or 30 µg (group IV) of VP6T or 10 µg VP6S (group VII). The VP6 adjuvant effect on NoV GII.4-specific blocking antibodies was investigated further. Human type A saliva and PGM were used as the HBGA sources for NoV GII.4 VLP binding. There was no VLP binding blocking ($BT_{50} = 25$) by the mouse sera immunized with the suboptimal 0·3 µg dose of VLP alone (Table 2). When VLPs were co-administered with 10 or 30 µg of VP6T or VP6S, BT_{50} of 100–200 were observed (Table 2). As expected, due to the lack of GII.4-specific serum antibodies, the 10 µg of VP6T

Table 2. Blocking antibody titres in immunized mouse sera

Group	Immunization	Saliva HBGA BT$_{50}$	PGM HBGA BT$_{50}$
I	0·3 µg VLP	25[a]	n.t.
II	0·3 µg VLP + 1 µg VP6T	50	50
III	0·3 µg VLP + 10 µg VP6T	200	200
IV	0·3 µg VLP + 30 µg VP6T	200	100
V	0·3 µg VLP + 10 µg VP6T (1 h)	50	50
VI	0·3 µg VLP + 10 µg VP6T (contralateral sites)	25	n.t.
VII	0·3 µg VLP + 10 µg VP6S	100	100
VIII	3 µg VLP	400	n.t.
IX (Ctrl)	Carrier only (PBS)	25	25

[a]BT_{50} of 25 was assigned to samples lacking blocking at a serum dilution 1:50.

HBGA = histo-blood group antigen; PGM = pig gastric mucin; BT_{50} = titres with 50% blocking of norovirus (NoV) GII.4-1999 VLP binding; VLP = virus-like particle; n.t. = not tested; VP6T = VP6 nanotubes; VP6S = VP6 nanospheres; Ctrl = control; PBS = phosphate-buffered saline.
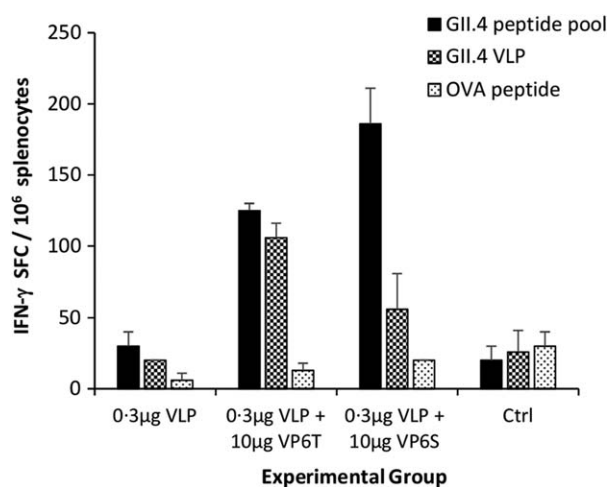
Fig. 4. Norovirus (NoV) GII.4-specific interferon (IFN)-γ production by T cells. NoV GII.4-1999-specific peptide pool, GII.4-1999 virus-like particles (VLPs) and ovalbumin (OVA) peptide (negative control) were used for stimulating IFN-γ production of the mice immunized with 0·3 μg VLP alone or co-administrated with 10 μg rVP6 nanotubes (VP6T) or nanospheres (VP6S). Negative control mice (Ctrl) were immunized with phosphate-buffered saline (PBS) only. Results are expressed as the mean spot-forming cells (SFC) per 10^6 splenocytes of the duplicate wells with standard errors of the mean. The experiments were repeated two or more times with similar results.

and 0·3 μg VLP administered at the contralateral site (group VI) as well as the control group (group IX) did not induce blocking antibodies (Table 2).

VP6 adjuvant effect on NoV-specific T cell responses

NoV GII.4-specific T cell responses were analysed by stimulating the splenocytes of immunized mice with GII.4-1999-specific peptide pool and GII.4-1999 VLPs and measuring IFN-γ production in the ELISPOT assay (Fig. 4). Immunization of mice with a 0·3 μg dose of GII.4 VLPs alone did not induce detectable IFN-γ production, but when co-administered with 10 μg of VP6T or VP6S a considerable NoV GII.4-specific IFN-γ secretion was observed (Fig. 4). There was no significant difference in the overall IFN-γ production by the T cells of mice immunized with VP6T or VP6S ($P > 0.05$). Mice immunized with the 10 μg of VP6T and 0·3 μg VLP at the contralateral sites (group VI, Table 1) were negative for all antigens tested in the ELISPOT IFN-γ (data not shown), confirming the local adjuvant effect of VP6 as seen for the NoV GII.4-specific antibody responses (Fig. 2a).

RV VP6-specific serum antibody responses

Each group of mice immunized with rVP6 (groups II–VII, Table 1) at different doses or different oligomeric structures developed RV VP6-specific serum IgG antibodies, indicating successful immunization (Fig. 5a). Interestingly, very

high VP6-specific IgG end-point titres (GMT 60887) were induced in mice immunized with GII.4 VLPs and VP6T at the contralateral sites (group VI, Table 1), ruling out the possibility that a lack of VP6 adjuvant effect observed in
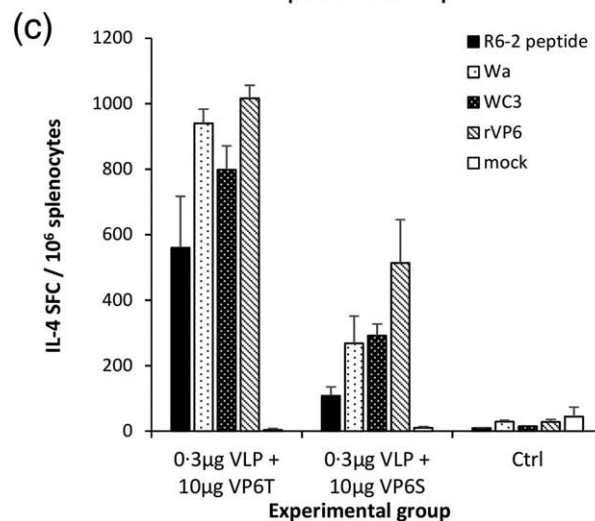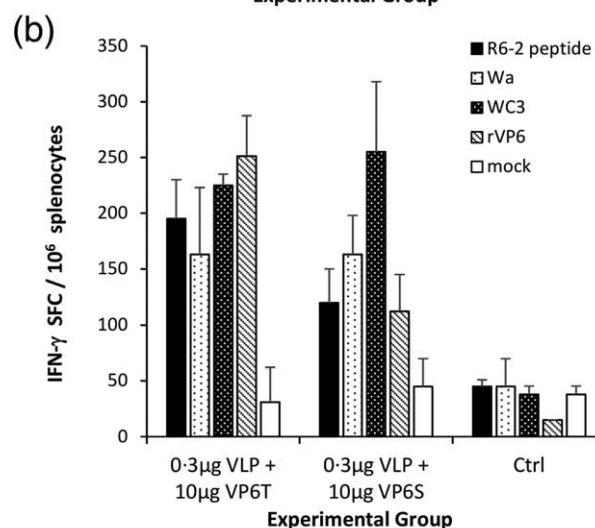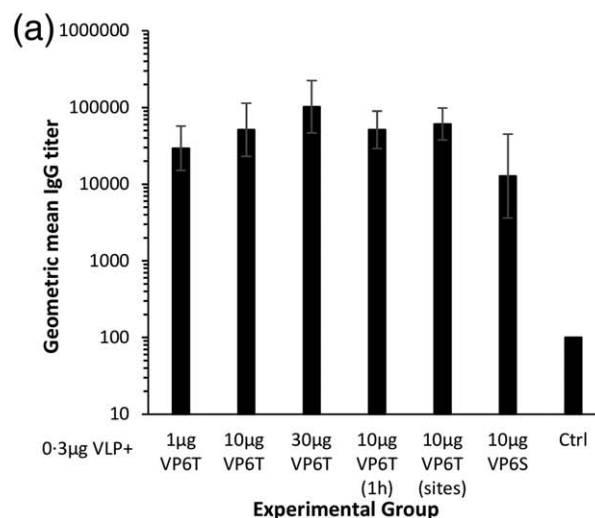
M. Malm *et al*.

Fig. 5. Rotavirus (RV) VP6-specific antibodies and T cell responses. VP6-specific immune responses were detected following immunization with 0·3 μg norovirus (NoV) GII.4 virus-like particles (VLPs) together with VP6 nanotubes (VP6T) or nanospheres (VP6S). Control (Ctrl) mice received phosphate-buffered saline (PBS) only. (a) Serum anti-VP6 IgG of individual mice were tested in enzyme-linked immunosorbent assay (ELISA) and the mean titration curves of each experimental group are shown. Bars represent log$_{10}$ geometric mean titres with 95% confidence intervals. For negative mice sera, an arbitrary titre of 1 : 100 (half the starting serum dilution, 1 : 200) was assigned. VP6-specific IFN-γ (b) and interleukin (IL)-4 (c) production by T cells was tested stimulating the cells with VP6-specific R6-2 peptide, RV Wa and WC3 cell culture antigens, mock antigen or recombinant VP6 protein (rVP6). Results are expressed as the mean spot-forming cells (SFC)/10^6 splenocytes of the duplicate wells with standard errors of the mean. The experiments were repeated two or more times with similar results.

this group might result from an unsuccessful immunization with rVP6.

RV VP6-specific T cell responses

ELISPOT IFN-γ (a hallmark of a Th1-type response) and IL-4 (a hallmark of a Th2-type response) were used to analyse RV VP6-specific T cell responses in splenocytes of immunized mice to VP6 derived R6-2 peptide epitope, RV cell culture antigens (Wa and WC3) or rVP6 protein. IFN-γ production to all antigens but to a mock antigen was detected in mice immunized by co-administration of 0·3 μg NoV GII.4 VLPs and 10 μg VP6T or VP6S (Fig. 5b). Immunization with VP6T induced somewhat higher IFN-γ production than VP6S, but the difference was not statistically significant ($P = 0.073$). When the same cells were tested for VP6-specific IL-4 production, a robust IL-4 response (up to 1016 SFC/10^6 cells) was observed in the group that received 0·3 μg NoV VLPs co-administered with 10 μg of VP6T (Fig. 5c). IL-4 production was also induced in the group that received 10 μg of VP6S (Fig. 5c) instead of VP6T; however, the response was significantly higher in the group that received VP6T ($P = 0.008$). No RV VP6-specific IFN-γ or IL-4 was secreted by the splenocytes of mice immunized with 0·3 μg GII.4 VLP alone (data not shown) or the control mice (Fig. 5b,c).

Discussion

We have demonstrated recently an *in-vivo* adjuvant effect of VP6T on the immunogenicity of NoV VLPs [17]. In addition, *in-vitro* studies have shown that VP6 induces APC activation and maturation [36]. In the present study, the mechanism of VP6 adjuvant action was investigated further to explore the effect of co-localization of the two antigens, NoV VLPs and rVP6, via co-delivery as a mixture

or as separate injections at the same or contralateral injection sites.

An adjuvant is defined as a compound that enhances the immune response to vaccine antigens. The adjuvants may be regarded as depots or vehicles or/and immunomodulatory agents. A depo effect facilitates and improves delivery of antigens to APCs. We therefore investigated if the VP6 functions as a carrier or delivery vehicle that would necessitate the VLP and rVP6 co-delivery as a mixture, instead of separate injections. The results demonstrated clearly that the adjuvant effect of VP6 is strictly dependent upon co-localization of the VP6 with NoV GII.4 VLPs. To accomplish the optimal rVP6 adjuvant effect on NoV VLP immunogenicity it was essential to co-administrate the VP6 with the NoV VLPs, as both temporal and spatial dissociation of VP6 and NoV VLPs impaired or completely abolished the adjuvant effect. A 1-h temporal difference in the administration of VP6T and NoV VLPs impaired the adjuvant effect dramatically, further supporting the role of rVP6 as a delivery vehicle. It has been published that particulate antigens travel very quickly, in terms of minutes, from the site of injection to the local lymphoid tissue [46]. Although this study does not extend to confirm this, the results suggest that RV VP6 and VLPs may form aggregates when co-formulated, VP6 functioning as a carrier. Indeed, our recently published results showed that NoV VLP uptake into the APCs was increased when mixed with the rVP6 [36].

In addition to acting initially as the delivery vehicle for NoV VLPs the VP6 adjuvant effect is probably enforced further by APC activation. After being delivered, rVP6 may induce local cytokine and chemokine production and activation and maturation of APC at the site, as shown by our earlier *in-vitro* studies [36]. Proinflammatory cytokines, such as tumour necrosis factor (TNF)-α, IL-6, IL-1 and granulocyte macrophage colony-stimulating factor (GM-CSF), enhance the adaptive immune response in several ways, including recruitment of APC at the site of injection, stimulating their maturation and migration to lymph nodes (LN) [47,48]. Therefore, the VP6 delivery probably leads to an increased number of NoV VLP-loaded APCs in the LN draining the injection site able to activate antigen-specific T cells. Three types of DCs, conventional and monocyte-derived in steady state skeletal muscles are targeted by i.m. immunization, which can encounter the antigen and migrate to LN [49]. Furthermore, VP6 activation of T cells in lymphoid tissues induces cytokine production by these cells, such as the observed IFN-γ, a Th1-type cytokine and IL-4, a Th2-type cytokine. Paracrine secretion of Th1 and Th2 cytokines by the VP6-specific T cells is of significance, as these cytokines drive proliferation and differentiation of co-delivered antigen; in this case NoV VLPs primed naive B and T lymphocytes into memory cells [50,51]. The localized nature of the VP6 adjuvanticity is supported by the observation

that VP6 administration at the contralateral site did not contribute to the NoV-specific immunity, even though high VP6-specific immune responses were observed. Moreover, serum collected at 3 and 24 h post-VP6T immunization was negative for proinflammatory cytokines TNF-α and IL-6 by ELISA (data not shown), arguing against a systemic adjuvant effect.

The results of the present study show that rVP6 promotes both Th1- and Th2-type responses to NoV without skewing the overall immune response in any particular direction. The adjuvants are mainly restricted to enhance either type of the responses, such as aluminium salts, which promote mainly Th2-type responses to the co-administered vaccine antigens [52]. The particle size and shape are shown to be central in the antigen internalization and transport to LN and immune cell activation [48,53–55]. Additionally, the particle size and shape may play a role in tuning the adaptive immunity, as rod-shaped particles have been reported to induce Th2-biased responses compared to spherical particles [56]. However, although we observed more IL-4 production by the VP6T-specific T cells compared to VP6S, both these nanostructures exerted a similar adjuvant effect on NoV GII.4-specific antibody responses.

Our results show, for the first time, the VP6 adjuvant effect on NoV-specific T cell immunity. It has been published that VP6 can potentiate the serum antibody response against RV in a mouse model by an intermolecular help mechanism [57]. In the present study, as the VP6 is not conjugated or linked to the VLPs, bystander T cell help is probably an important mechanism. These cells may drive proliferation and differentiation of NoV-antigen primed B and T lymphocytes into memory cells and antibody-secreting plasma cells either by cell-to-cell contact (CD40-CD40L interaction) [58] or soluble cytokine production [59].

Altogether, this study shows clearly that co-administration of the VP6 with NoV VLPs is essential for the optimal adjuvant effect on NoV-specific immune responses and that the VP6 acts as a delivery vehicle as well as immunomodulator. Safety is a major concern when it comes to adjuvant approval for human use, especially for healthy infants [16]. The results of this study support the use of rVP6 not only to provide protection against RV in the proposed NoV VLP–RV VP6 combination vaccine [9,10], but also as an adjuvant to potentiate the NoV VLP immunogenicity.

Acknowledgements

Author contributions

M. M. conducted immunizations, sample acquisition and processing and laboratory analysis, including data acquisition, analysis and interpretation (ELISA, blocking assays), writing the manuscript and final approval of the version to be submitted. S. H. conducted immunizations, sample acquisition, processing and laboratory analysis, data acquisition and analysis (protein and virus production, ELISPOT assays). Final approval of the version to be submitted. T. V. is the head of the Vaccine Research Center and conducted critical review of the paper and gave final approval of the version to be submitted. V. B. is the head of the laboratory and corresponding author, and conducted the conception and designing the study, data interpretation, drafting and writing the paper, critical revision of the paper for important intellectual content and final approval of the version to be submitted.

Disclosure

All the authors declare no disclosures.

References

1 Puustinen L, Blazevic V, Salminen M, Hämäläinen M, Räsänen S, Vesikari T. Noroviruses as a major cause of acute gastroenteritis in children in Finland, 2009–2010. Scand J Infect Dis 2011; **43**:804–8.

2 Patel MM, Steele D, Gentsch JR, Wecker J, Glass RI, Parashar UD. Real-world impact of rotavirus vaccination. Pediatr Infect Dis J 2011; **30**:S1–5.

3 Dennehy PH. Viral gastroenteritis in children. Pediatr Infect Dis J 2011; **30**:63–4.

4 Jiang X, Wang M, Graham DY, Estes MK. Expression, self-assembly, and antigenicity of the Norwalk virus capsid protein. J Virol 1992; **66**:6527–32.

5 Vesikari T. Rotavirus vaccination: a concise review. Clin Microbiol Infect 2012; **18** (Suppl 5):57–63.

6 Desselberger U. Rotaviruses. Virus Res 2014; **190**:75–96.

7 Buttery JP, Danchin MH, Lee KJ et al. Intussusception following rotavirus vaccine administration: post-marketing surveillance in the National Immunization Program in Australia. Vaccine 2011; **29**:3061–6.

8 Donato CM, Ch'ng LS, Boniface KF et al. Identification of strains of RotaTeq rotavirus vaccine in infants with gastroenteritis following routine vaccination. J Infect Dis 2012; **206**:377–83.

9 Blazevic V, Lappalainen S, Nurminen K, Huhti L, Vesikari T. Norovirus VLPs and rotavirus VP6 protein as combined vaccine for childhood gastroenteritis. Vaccine 2011; **29**:8126–33.

10 Okada M, Mukai A, Nishino T, Arinobu D, To H, Satoh M. Purification method for virus-like particles. 2013. Patent application no. 2013-146240. Japan Patent Office, Japan.

11 Tamminen K, Lappalainen S, Huhti L, Vesikari T, Blazevic V. Trivalent combination vaccine induces broad heterologous immune responses to norovirus and rotavirus in mice. PLOS ONE 2013; **8**:e70409.

12 Lappalainen S, Tamminen K, Vesikari T, Blazevic V. Comparative immunogenicity in mice of rotavirus VP6 tubular structures and virus-like particles. Hum Vaccin Immunother 2013; **9**:1991–2001.

13 Lappalainen S, Pastor AR, Malm M *et al*. Protection against live rotavirus challenge in mice induced by parenteral and mucosal delivery of VP6 subunit rotavirus vaccine. Arch Virol 2015; **160**: 2075–8.

14 Perrie Y, Mohammed AR, Kirby DJ, McNeil SE, Bramwell VW. Vaccine adjuvant systems: enhancing the efficacy of sub-unit protein antigens. Int J Pharm 2008; **364**:272–80.

15 Petrovsky N, Aguilar JC. Vaccine adjuvants: current state and future trends. Immunol Cell Biol 2004; **82**:488–96.

16 Baylor NW, Egan W, Richman P. Aluminum salts in vaccine – US perspective. Vaccine 2002; **20** (Suppl 3):S18–23.

17 Blazevic V, Malm M, Arinobu D, Lappalainen S, Vesikari T. Rotavirus capsid VP6 protein acts as an adjuvant *in vivo* for norovirus virus-like particles in a combination vaccine. Hum Vaccin Immunother 2015; **12**:740–8.

18 Prasad BV, Wang GJ, Clerx JP, Chiu W. Three-dimensional structure of rotavirus. J Mol Biol 1988; **199**:269–75.

19 Offit PA, Blavat G. Identification of the two rotavirus genes determining neutralization specificities. J Virol 1986; **57**:376–8.

20 Svensson L, Sheshberadaran H, Vene S, Norrby E, Grandien M, Wadell G. Serum antibody responses to individual viral polypeptides in human rotavirus infections. J Gen Virol 1987; **68**: 643–51.

21 Franco MA, Angel J, Greenberg HB. Immunity and correlates of protection for rotavirus vaccines. Vaccine 2006; **24**:2718–31.

22 Estes MK, Kapikian AZ. Rotaviruses In: Knipe DMHP, ed. Field's virology. Philadelphia, PA: Lippincott Williams & Wilkins, 2007:1917–74.

23 Tang B, Gilbert JM, Matsui SM, Greenberg HB. Comparison of the rotavirus gene 6 from different species by sequence analysis and localization of subgroup-specific epitopes using site-directed mutagenesis. Virology 1997; **237**:89–96.

24 Estes MK, Crawford SE, Penaranda ME *et al*. Synthesis and immunogenicity of the rotavirus major capsid antigen using a baculovirus expression system. J Virol 1987; **61**:1488–94.

25 Lepault J, Petitpas I, Erk I *et al*. Structural polymorphism of the major capsid protein of rotavirus. EMBO J 2001; **20**:1498–507.

26 Li T, Lin H, Zhang Y *et al*. Improved characteristics and protective efficacy in an animal model of *E. coli*-derived recombinant double-layered rotavirus virus-like particles. Vaccine 2014; **32**: 1921–31.

27 Bugli F, Caprettini V, Cacaci M *et al*. Synthesis and characterization of different immunogenic viral nanoconstructs from rotavirus VP6 inner capsid protein. Int J Nanomedicine 2014; **9**: 2727–39.

28 Mathieu M, Petitpas I, Navaza J *et al*. Atomic structure of the major capsid protein of rotavirus: implications for the architecture of the virion. EMBO J 2001; **20**:1485–97.

29 Ward RL, McNeal MM. VP6: a candidate rotavirus vaccine. J Infect Dis 2010; **202** (Suppl):S101–7.

30 Redmond MJ, Ohmann HB, Hughes HP *et al*. Rotavirus particles function as immunological carriers for the delivery of peptides from infectious agents and endogenous proteins. Mol Immunol 1991; **28**:269–78.

31 Peralta A, Molinari P, Taboga O. Chimeric recombinant rotavirus-like particles as a vehicle for the display of heterologous epitopes. Virol J 2009; **6**:192.

32 Istrate C, Douagi I, Charpilienne A *et al*. Bone marrow dendritic cells internalize live RF-81 bovine rotavirus and rotavirus-like particles (RF 2/6-GFP-VLP and RF 8*2/6/7-VLP) but are only activated by live bovine rotavirus. Scand J Immunol 2007; **65**:494–502.

33 Rodriguez M, Wood C, Sanchez-Lopez R, Castro-Acosta RM, Ramírez OT, Palomares LA. Understanding internalization of rotavirus VP6 nanotubes by cells: towards a recombinant vaccine. Arch Virol 2014; **159**:1005–15.

34 Pan X-X, Zhao B-X, Teng Y-M *et al*. Immunoreactivity of chimeric proteins carrying poliovirus epitopes on the VP6 of rotavirus as a vector. Mol Biol 2016; **50**:731–9.

35 Palmieri V, Bugli F, Papi M *et al*. VP6-SUMO self-assembly as nanocarriers for gastrointestinal delivery. J Nanomater 2015; **2015**: Article ID 378786.

36 Malm M, Tamminen K, Lappalainen S, Vesikari T, Blazevic V. Rotavirus recombinant VP6 nanotubes act as an immunomodulator and delivery vehicle for norovirus virus-like particles. J Immunol Res 2016; **2016**:9171632.

37 Huhti L, Blazevic V, Nurminen K, Koho T, Hytönen VP, Vesikari T. A comparison of methods for purification and concentration of norovirus GII-4 capsid virus-like particles. Arch Virol 2010; **155**:1855–8.

38 Lappalainen S, Vesikari T, Blazevic V. Simple and efficient ultrafiltration method for purification of rotavirus VP6 oligomeric proteins. Arch Virol 2016; **161**:3219–23.]

39 Malm M, Tamminen K, Vesikari T, Blazevic V. Type-specific and cross-reactive antibodies and T cell responses in norovirus VLP immunized mice are targeted both to conserved and variable domains of capsid VP1 protein. Mol Immunol 2016; **78**:27–37.

40 McNeal MM, Basu M, Bean JA, Clements JD, Choi AH, Ward RL. Identification of an immunodominant CD4+ T cell epitope in the VP6 protein of rotavirus following intranasal immunization of BALB/c mice. Virology 2007; **363**:410–8.

41 Tamminen K, Huhti L, Koho T *et al*. A comparison of immunogenicity of norovirus GII-4 virus-like particles and P-particles. Immunology 2012; **135**:89–99.

42 Lindesmith LC, Debbink K, Swanstrom J *et al*. Monoclonal antibody-based antigenic mapping of norovirus GII.4-2002. J Virol 2012; **86**:873–83.

43 Harrington PR, Lindesmith L, Yount B, Moe CL, Baric RS. Binding of Norwalk virus-like particles to ABH histo-blood group antigens is blocked by antisera from infected human volunteers or experimentally vaccinated mice. J Virol 2002; **76**: 12335–43.

44 Uusi-Kerttula H, Tamminen K, Malm M, Vesikari T, Blazevic V. Comparison of human saliva and synthetic histo-blood group antigens usage as ligands in norovirus-like particle binding and blocking assays. Microbes Infect 2014; **16**:472–80.

45 Malm M, Uusi-Kerttula H, Vesikari T, Blazevic V. High serum levels of norovirus genotype-specific blocking antibodies correlate with protection from infection in children. J Infect Dis 2014; **210**:1755–62.

46 Young KR, Arthus-Cartier G, Yam KK *et al*. Generation and characterization of a trackable plant-made influenza H5 virus-like particle (VLP) containing enhanced green fluorescent protein (eGFP). FASEB J 2015; **29**:3817–27.

47 Stoitzner P, Zanella M, Ortner U *et al*. Migration of Langerhans cells and dermal dendritic cells in skin organ cultures: augmentation by TNF-alpha and IL-1beta. J Leukoc Biol 1999; **66**:462–70.

48 Manolova V, Flace A, Bauer M, Schwarz K, Saudan P, Bachmann MF. Nanoparticles target distinct dendritic cell populations according to their size. Eur J Immunol 2008; **38**:1404–13.

49 Langlet C, Tamoutounour S, Henri S *et al.* CD64 expression distinguishes monocyte-derived and conventional dendritic cells and reveals their distinct role during intramuscular immunization. J Immunol 2012; **188**:1751–60.

50 Jordan MB, Mills DM, Kappler J, Marrack P, Cambier JC. Promotion of B cell immune responses via an alum-induced myeloid cell population. Science 2004; **304**:1808–10.

51 Paul WE, Zhu J. How are T(H)2-type immune responses initiated and amplified? Nat Rev Immunol 2010; **10**:225–35.

52 Marrack P, McKee AS, Munks MW. Towards an understanding of the adjuvant action of aluminium. Nat Rev Immunol 2009; **9**:287–93.

53 Champion JA, Mitragotri S. Role of target geometry in phagocytosis. Proc Natl Acad Sci USA 2006; **103**:4930–4.

54 Irvine DJ, Swartz MA, Szeto GL. Engineering synthetic vaccines using cues from natural immunity. Nat Mater 2013; **12**:978–90.

55 Benson RA, MacLeod MK, Hale BG, Patakas A, Garside P, Brewer JM. Antigen presentation kinetics control T cell/dendritic cell interactions and follicular helper T cell generation *in vivo*. Elife 2015; **4**.

56 Kumar S, Anselmo AC, Banerjee A, Zakrewsky M, Mitragotri S. Shape and size-dependent immune response to antigen-carrying nanoparticles. J Control Release 2015; **220**:141–8.

57 Esquivel FR, Lopez S, Guitierrez XL, Arias C. The internal rotavirus protein VP6 primes for an enhanced neutralizing antibody response. Arch Virol 2000; **145**:813–25.

58 VanCott JL, McNeal MM, Flint J, Bailey SA, Choi AH, Ward RL. Role for T cell-independent B cell activity in the resolution of primary rotavirus infection in mice. Eur J Immunol 2001; **31**:3380–7.

59 Diehl S, Rincon M. The two faces of IL-6 on Th1/Th2 differentiation. Mol Immunol 2002; **39**:531–6.